Journal of Nonlinear and Convex Analysis
Volume 26, Number 7, 2025, 1999–2014

Yokohama Publishers
ISSN 1880-5221 ONLINE JOURNAL

DYNAMIC RELIABILITY ANALYSIS OF THE UNDER-CONSTRUCTION TRANSMISSION TOWER STRUCTURE UNDER STRONG CONVECTIVE AND EXTREME WINDY CONDITIONS

XIAOFAN LIU*, TAO HUANG, ZHIWEI LIU, AND JIAO ZHU

Abstract. Strong convective weather often occurs in Jiangsu, an eastern province of China, and is most typical of downbursts. The sudden and highly destructive downbursts would pose serious threats to the transmission tower-line system. In this study, the instantaneous wind speed and wind-induced loads acting on the transmission tower in downbursts were introduced and the random distribution characteristic of downburst wind speed was examined and described by Fréchet distribution. Using the reliability theory, a failure probability model expressed by the displacement failure in the pole was established by considering three performance levels and their corresponding limit states (LS). At a 90o direction angle of downburst winds, a case study related to the dynamic failure probability in terms of the pole displacement was conducted on an under-construction tower-pole system derived from a 500 kV transmission tower in Jiangsu Province. Results show that under downbursts the displacement responses in the tower-pole system are more remarkable than the stress responses, especially for the suspension pole. For three LSs, the failure probabilities occurred in the pole present different growth levels as the maximum wind speed of Vmax increases from 25 m/s to 55 m/s. At the extreme wind speed of 55 m/s, the failure probabilities for LS1, LS2, and LS3 reach 39%, 33%, and 4%, respectively, for the pole with a vertical length of 28 m and a working height of 20 m. Increasing the cross-sectional area of the elements is a more effective way to enhance the wind resistance of the pole than decreasing its vertical length. Above findings could provide a valuable reference for the failure risk analysis of an under-construction tower-pole system suffering from strong convective weathers.

1. Introduction

The southeastern coastal region is one of the more developed socio-economic areas in China, with a high demand for electricity. At same time, strong convective and windy weathers occur frequently in these areas. Transmission towers are different from general civil engineering structures in that they have the characteristics of light weight and high flexibility. They are very sensitive to wind loads and prone to significant dynamic response under strong winds [2, 9, 19, 26]. Previous disasters have shown that convective winds, strong winds, and typhoons are the

2020 *Mathematics Subject Classification.* 90C35, 93C41, 68U35, 62H25.

Key words and phrases. Strong convective weather, under-construction transmission tower, downburst, wind vibration response, failure probability.

This research is financially supported by State Grid Jiangsu Electric Power Co., Ltd., China (No. J2023090).

*Corresponding author.

main causes of transmission towers' damage and collapse accidents in coastal areas [4,16,18,23,26]. In addition, during the construction period of these transmission towers, they may also experience varying degrees of strong convective and windy weather. Considering the imperfect structural characteristics and tower assembly process during construction, it is also of great significance to conduct construction safety assessments of transmission towers suffering from strong convective and windy loads. Under strong convective and extreme windy conditions, the dynamic response and safety assessments of transmission towers and tower-line systems have received widespread attention from scholars all over the world. Wang et al. [25] proposed a nonlinear analytical model to predict the quasi-static vibration responses of a multi-span transmission line-insulator system under moving downbursts. Fang et al. [9] carried out nonlinear dynamic analysis with an ANSYS model to study the wind-induced responses of a transmission tower and its tower-line system under downburst and found that the storm moving speed had little effect on the system response induced by wind loads. The numerical simulation results got from Zheng and Fan [28] indicated that the fully coupled dynamic analysis could effectively capture the nonlinear behaviors of towers under downburst wind loads and the progressive collapse of a tower-line system was significantly affected by the wind speed and movement path of downbursts. Ahmed and Damatty [1] conducted nonlinear dynamic analysis utilizing a computational fluid dynamics (CFD) model to identify the thunderstorm-related cascade failure of the transmission tower lines under downburst wind loads. In the study conducted by Zhang and Xie [26], the static and dynamic analyses were utilized to estimate the wind load capacity of a transmission tower based on the field investigations. They proposed that the dynamic analysis should be incorporated in the wind-induced failure analysis of transmission towers. Similarly, Zhu et al. [29] adopted the static nonlinear analysis and dynamic analysis to determine the threshold and maximum displacements of a transmission tower under strong wind respectively and then assessed the wind-induced failure probability of the tower considering the wind attack angles. Tian et al. [23] completed the full-scale tests and numerical simulations to explore the failure mechanism of a latticed steel tubular transmission tower exposed to extreme wind loads and found that the tower collapse under strong wind condition would mainly be attributed to the buckling failures occurred in leg members. Shehata and Damatty [22] analyzed the cascade failure of the transmission tower-line system under strong winds induced by downbursts using a numerical model. Based on the catenary approach, they also analyzed the failure of the transmission line's conductors under downbursts [21]. Considering the combined effect of wind speed and direction, Bi et al. [4] evaluated the wind-induced failure probability of a transmission tower-line system and proposed that the joint probability distribution should be incorporated to obtain a reliable failure assessment. Similar investigations on the fragility and failure evaluation of transmission tower or tower-line system have also completed in recent years considering the actions of extreme winds or downbursts [20,27,30]. All above studies could provide valuable references for strong wind-induced vibration response and failure analysis of transmission towers. However, few research has been conducted to evaluate the safety and reliability of under-construction transmission towers when they suffer from severe winds. Therefore, more attention should be paid to this

overlooked issue. In this paper, the downburst was selected as a typical example to exhibit extreme wind fields to an under-construction transmission tower. The instantaneous wind speed and wind load induced by downbursts were simulated. Considering the characteristics of random variations in wind speed, material, and geometric dimension, the probability distribution models and the displacement related failure probability models were established using reliability theory. Finally, the failure probabilities under three different performance levels were discussed on an under-construction transmission tower-pole system suffering from the action of downbursts. Analytical results could provide useful references for effectively evaluating the ability to resist the strong windy weather and reducing the failure risk of these under-construction transmission towers.

2. Wind load simulation under downbursts

Among the severe convective and windy conditions, downbursts accompanied by thunderstorms have become the typical strong wind weather and caused huge damage to the transmission tower-line systems [1, 22, 28]. The downburst induced winds are usually characterized by local effect, short term, and destructive high intensity [8]. In this study, the extreme wind appeared in downbursts was introduced and the corresponding loads acting on the under-construction transmission tower were simulated and calculated.

2.1. **Wind field of downbursts.**

According to the definition of winds in downbursts, its instantaneous wind speed $U(z,t)$ at height z and time t could be described as Eq. (2.1) [7, 28].

$$U(z,t) = V(z)f(t) + u(z,t) \tag{2.1}$$

where, V(z) is the vertical profile of maximum mean wind speed in downburst; $f(t)$ is a time related function with a value in the range of $0 \sim 1$ and $u(z,t)$ is the downburst fluctuating wind speed. The calculation expression shown in Eq. (2.2) is utilized here to determine $V(z)$ [24] and its variations with increasing height z under the determined conditions of $z_{\max} = 50$ m and $V_{\max} = 30 \sim 50$ m/s are depicted in Figure 1. For $u(z,t)$, it can be expressed with a product of an amplitude modulation function and a random process [4, 19], as shown in Eq.(3.3).

$$V(z) = 1.22\left[e^{\left(-\frac{0.15z}{z_{\max}}\right)} - e^{\left(-\frac{3.2175z}{z_{\max}}\right)}\right]V_{\max} \tag{2.2}$$

where, $V_{\max}$ is the maximum wind speed at the profile of $V(z)$ and $z_{\max}$ is the height to achieve $V_{\max}$.

$$u(z,t) = a(z,t)k(z,t) \tag{2.3}$$

where, $a(z,t)$ is an amplitude modulation function, which can be approximately assumed to be $(0.08 - 0.11)V(z)f(t)$ [7]; $k(z,t)$ is a stationary Gaussian random process with a zero mean and a variance of 1, which can be calculated by the Kaimal spectrum [7, 28]. Using the power spectral density curve, Figure 2 presents the relation between Kaimal spectrum and power spectral of this Gaussian random process calculated at the centroid position of the transmission tower at a height

of 30 m. By comparison, it is evident that the Kaimal spectrum can effectively simulate the fluctuating wind speed of downburst.

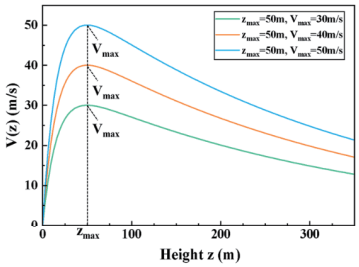

FIGURE 1. Vertical wind speed profiles of downbursts.

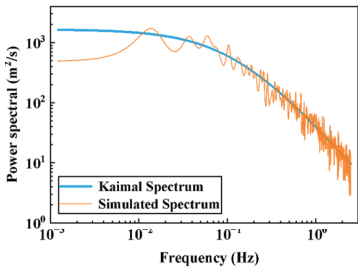

FIGURE 2. Comparison of simulated spectrum with Kaimal Spectrum.

Considering a downburst with a radial distance of 1000 m and a maximum radial wind speed of 45 m/s, the time histories of mean wind speed with $V_{\max} = 40m/s$ and $z_{\max} = 50m$, fluctuating wind speed and instantaneous wind speed can be achieved at any height using Eqs. (2.1)–(2.3). The demonstration wind speed-time histories at a height of 38 m are presented in Figure 3.

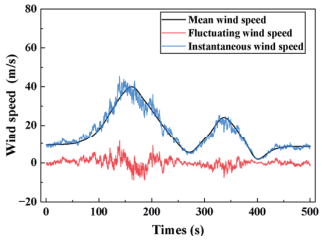

FIGURE 3. Downburst wind speed-time histories at a height of 38 m.

2.2. **Wind load of downbursts.** According to the guidelines suggested by CSA [5] and ASCE [3], the downburst wind forces acting at two loading panels in the X- and Y-direction, Fx and Fy, can be calculated by Eq. (2.4) and Eq. (2.5), respectively.

$$F_x = \frac{1}{2}\rho U^2 \cos^2\alpha\, C_{rx} A_x, \tag{2.4}$$

$$F_y = \frac{1}{2}\rho U^2 \sin^2\alpha\, C_{ry} A_y \tag{2.5}$$

where, ρ is the air density with $\rho = 1.29kg/m3$; U is the downburst wind speed determined by Eq. (2.1); α is the direction angle of wind speed corresponding to X-direction; C_{rx} and C_{ry} are the resistance coefficients in X- and Y-direction, respectively; A_x and A_y are the windshield areas of the transmission tower in X- and Y-direction, respectively.

3. Reliability analysis of under-construction tower-pole system under downbursts

3.1. **Probability distributions.**

3.1.1. *Wind speed of downbursts.* As shown in Figure 3, the wind speed appeared in downbursts presents significant uncertainty. Therefore, wind speed should be treated as a random variable in the reliability analysis for the transmission tower suffering from strong winds [4]. Using the simulation method for wind speeds, the wind speed-time histories of a downburst were computed over a period of 500 seconds for various values of $V_{\max}$ utilizing MATLAB. The typical results are statistically analyzed for frequency distribution within a wind speed range of 0-70 m/s, as shown in Figure 4, and the non-linear curve fittings are performed on the statistical results. Three commonly utilized wind speed variable probability models, including Weibull, Gumbel and Fréchet distributions [4], are employed to try to fit the probability density of wind speed, as illustrated in Figure 4. Comparing with the fitting results of above three distributions, it can be observed that the Fréchet distribution exhibits a closer alignment with the frequency distribution histogram, indicating that the Fréchet distribution could present a better model to describe the probability density of downburst wind speed. Taking $V_{\max} = 50m/s$ for an example, the corresponding expressions of three probability density functions can be constructed according to the formulas presented in Table 1. Finally, the probability density function of downburst wind speed can be approximately expressed using Fréchet distribution as Eq. (3.1).

$$f(v) = \frac{2.48}{8.98}\left(\frac{v}{8.98}\right)^{(2.48-1)} \cdot e^{-\left(\frac{v}{8.98}\right)^{2.48}}, \quad v > 0. \tag{3.1}$$

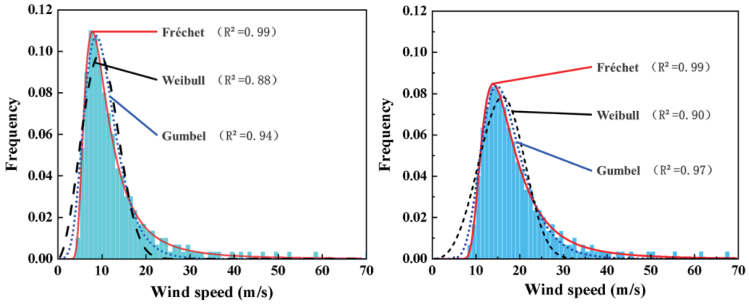

(A) $V_{\max} = 40m/s$ (B) $V_{\max} = 50m/s$

Figure 4. Probability distribution of downburst wind speed.

3.1.2. *Material and geometric dimension.* For a transmission tower under construction, the main materials utilized in the tower-pole system are the angle steel and steel pipe elements with a strength grade of Q345. The China Standard of GB 50068-2018 [11] suggests that the probability distribution of material strength should adopt normal distribution or logarithmic normal distribution, and the standard value of material strength should be determined by the 0.05th percentile of its probability

TABLE 1. Fitting results of probability distribution at $V_{\max} = 50m/s$.

Probability distribution	pdf $f(v)$	Regression coefficients					R^2	RMSE
		μ	α	β	k	λ		
Gumbel	$\frac{1}{\beta}e^{-(v-\mu)/\beta}\cdot e^{-e^{-(v-\mu)/\beta}}$	3.42	-	2.53	-	-	0.94	0.006
Weibull	$\frac{\alpha}{\beta}(\frac{v}{\beta})^{(-1-\alpha)}\cdot e^{-(\frac{v}{\beta})^{-\alpha}}$	-	2.76	11.12	-	-	0.88	0.011
Fréchet	$\frac{k}{\lambda}\left(\frac{v}{\lambda}\right)^{(k-1)}\cdot e^{-\left(\frac{v}{\lambda}\right)^{k}}$	-	-	-	2.48	8.98	0.99	0.007

distribution. Accordingly, the relations between the standard value f_k and the mean value μ_f can be described by Eq. (3.2) or Eq. (3.3) when the probability distribution of material strength follows normal distribution or logarithmic normal distribution, respectively. In addition, the probability distribution of geometric dimension, such as the limb thickness and width of angle steel, and the thickness of steel pipe, can be usually assumed to comply with normal distribution. According to the previous studies [4, 13, 17], the statistical parameters of material and geometric dimension of angle steel and steel pipe are summarized in Table 2.

$$f_k = \mu_f - 1.645\sigma_f, \tag{3.2}$$

$$f_k = \mu_f \exp(-1.645\delta_f), \tag{3.3}$$

where, σ_f and δ_f are standard deviation and coefficient of variation (COV) of a random variable, respectively.

TABLE 2. Statistical parameters of material and geometric dimensions.

Parameter	μ_f	σ_f	δ_f	Distribution
Elastic modulus of steel, E_s/GPa	206	6.18	0.03	Logarithmic normal distribution
Poisson's ratio of steel, v	0.3	0.009	0.03	Logarithmic normal distribution
Yield strength of Q345, f_y/MPa	387.1	27.10	0.07	Logarithmic normal distribution
Limb thickness of angle steel/mm	$0.985f_k$	-	0.032	Normal distribution
Limb width of angle steel/mm	$1.001f_k$	-	0.008	Normal distribution
Thickness of steel pipe/mm	$0.985f_k$	-	0.032	Normal distribution
Vertical length of pole/m	28	1.4	0.05	Normal distribution

3.2. **Probabilistic model of wind-induced displacement.** For an under-construction tower-pole system suffering from extreme wind loads, the displacement failure in the pole is usually more significant than the strength failure appeared in the tower. Therefore, the maximum displacement angle occurred in the pole can be utilized as a quantitative index to judge the damage and failure degrees of the

transmission tower-pole system. The maximum displacement angle (MDA) of the pole can be expressed as:

$$MDA = \frac{\Delta_{\max}}{h} \tag{3.4}$$

where, $\Delta_{\max}$ is the maximum displacement in the pole; and h is the vertical length of the pole. As mentioned above, the parameters affecting the displacement response of tower and pole elements under wind loads, mainly including wind speed and direction, material's physical and mechanical properties, and geometric dimensions of steel elements, exhibit uncertainty or random nature. Using the probability density functions of these random variables displayed in Table 1 and Table 2, the cumulative distribution function (CDF) of the maximum displacement $\Delta_{\max}$ can be described as:

$$F_\delta(\Delta_{\max}) = \Pr\{\delta \le \Delta_{\max}\} = \int_{\delta \le \Delta_{\max}} f(\bar{X})\, d\bar{X} \tag{3.5}$$

where, $\bar{X} = (X_1, X_2, \ldots, X_n)^T$ is the random variable vector; and $f(\bar{X})$ is the joint probability density function of the vector $\bar{X}$.

3.3. **Functional function and failure probability.** In order to quantify the failure risk of wind-induced displacement on the overall incomplete tower-pole system, the functional functions which can express the serviceability limit state in terms of displacement should be established according to failure determination of both tower and pole. Based on previous disaster examples and research results on the failure patterns of transmission towers [6, 10], the damage degree of under-construction tower-pole system can be qualitatively described as three successive states, as listed in Table 3. The corresponding performance levels (PL) can be expressed as $0.8[\mathrm{DA}] \le \mathrm{MDA} < [\mathrm{DA}]$, $[\mathrm{DA}] \le \mathrm{MDA} < 1.3[\mathrm{DA}]$ and $\mathrm{MDA} \ge 1.3[\mathrm{DA}]$, respectively. Thus, three limit states (LS) and their related functional functions can be formulated as follows:

$$g(\bar{X}) = \begin{cases} g_1(\bar{X}) = 0.8[\mathrm{DA}] - \mathrm{MDA}(X_1, X_2, \ldots, X_n), \\ g_2(\bar{X}) = 1.0[\mathrm{DA}] - \mathrm{MDA}(X_1, X_2, \ldots, X_n), \\ g_3(\bar{X}) = 1.3[\mathrm{DA}] - \mathrm{MDA}(X_1, X_2, \ldots, X_n) \end{cases} \tag{3.6}$$

where, [DA] is the limited displacement angle, which can be assumed to be 1/75 in accordance with Chinese standard of GB 50135-2019 [28]; $\mathrm{MDA}(X_1, X_2, \ldots, X_n)$ is the maximum displacement angle occurred in the pole under practical wind loads.

TABLE 3. Qualitative description of damage state.

Limit state	Faulted condition	State description	Performance level
LS1	Minor harm	System can continue to be used after few maintenances.	$0.8[DA] \le MDA < [DA]$
LS2	Serious harm	System has nonlinear deformation and needs a lot of maintenance to be reused.	$[DA] \le MDA < 1.3[DA]$
LS3	Complete harm	System is unusable and deemed damaged.	$MDA \ge 1.3[DA]$

According to the reliability theory, the failure probability in terms of pole displacement can be calculated by Eq. (3.7). Several techniques and methods can be utilized for probability assessment. However, it is considered that in this case the non-linear nature of limit state function indicates that analysis through a Monte Carlo technique is likely to be the most efficient approach.

$$p_{f_i} = \Pr\{g_i(\bar{X}) < 0\} = \int_{g_i(\bar{X})<0} f(\bar{X})\, d\bar{X}, \quad (i = 1, 2, 3). \tag{3.7}$$

4. Case study

4.1. **Finite element model of transmission tower-pole system.** In this study, a transmission tower under construction in the Yixu 500 kV transmission line located at southeastern coastal region of Jiangsu Province is employed as the example to demonstrate the reliability analysis under extreme wind conditions induced by downbursts. A tower-pole system is utilized to construct the transmission tower, as shown in Figure 5 (a), and its total height is 50.8 m. It can be observed from Figure 5 (a) that the pole is supported by ropes at the bottom and tensioned by the cables at the top. The main materials and elements used in the tower body and the pole with a vertical length of 28 m are listed in Table 4.

Table 4. Material and dimension parameters.

Object	Element	Strength grade	Dimension	Yield strength f_{yk} (MPa)	Elastic modulus, E_s (GPa)	Sectional area (mm^2)
Tower	Angle steel	Q235	L40*4-L63*5	235	210	320-630
		Q345	L75*6-L160*12	345	210	900-3840
		Q420	L180*14-L200*20	420	210	5040-8000
Pole	Steel pipe	Q345	Φ50×3 Φ32×2.5	345	210	300 160
	Supporting rope	Φ^S	ϕ21.6	1860	215	380
	Tensioned cable	Φ^S	Φ17.8	1860	215	260

Considering the working height of the tower-pole system and the height $z_{\max}$ corresponding to maximum wind speed $V_{\max}$ in downbursts simultaneously, the construction condition with a working height of 30 m defined at the bottom of the pole is chosen as a typical case. Accordingly, a finite element (FE) model of this tower-pole system is established using ABAQUS software and illustrated in Figure 5 (b). In this FE model, the angle steel elements adopted in the tower body and the steel pipe elements used in the pole are built with the T3D2 truss elements. Their constitutive model in axial loading is the ideal elastic-plastic model with an elastic modulus of 2.1 × 105MPa and a Poisson's ratio of 0.3. To achieve the tensioning state in the supporting ropes and cables, a 'cooling method' is utilized to generate prestressing forces in them. The foot of tower body is set with rigid connections and the both ends of tensioned cables are set as hinge joints. Besides, the both ends of supporting ropes are configured with PIN coupling connections, allowing for the free rotation at hinge joints.

At a 90° direction angle, the wind induced loads are simply treated as concentrated forces acting on the main elements of the tower-pole system with an interval of 5 m [9, 28], as depicted in Figure 5 (b). A nonlinear implicit dynamic method is applied in the calculation using ABAQUS software, which can accurately simulate the dynamic characteristics of the established model. By applying quasi-static equivalent wind loads, the displacement responses of this tower-pole system were identified under the condition of extreme wind caused by downbursts. Accordingly, the whole failure state of the tower-pole system was assessed during different construction phases under various variable parameters.

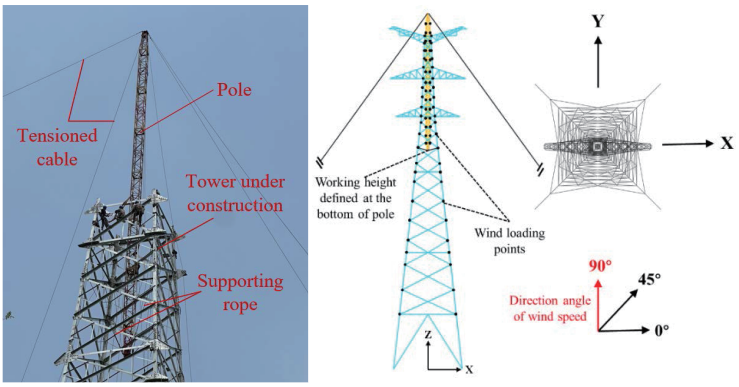

(A) Main elements (B) FE model

FIGURE 5. Transmission tower-pole system under construction.

4.2. **Results and discussion.** During calculation, the Latin Hypercube Sampling (LHS) method is employed to sample the random variables utilized here, allowing for a more efficient and accurate estimation of the failure probability [4, 6, 29]. To address this issue in this study, a total of 300 wind speed samples are constructed using this method, and each sample is analyzed individually. Besides, the effects of working height, dimension, and sectional area of the pole on the displacement related failure are particularly considered and illustrated in this work. The typical displacement failure states of the pole are illustrated in Figure 6. Besides, the wind-induced responses of the tower-pole system will constantly change as the tower construction progresses. Table 5 shows the maximum stress and displacement results of the system with increasing the working height of pole from 15 m to 32 m. It can be observed that under downbursts the displacement responses in the tower-pole system are more remarkable than the stress responses, especially for the suspension pole.

4.2.1. *Effect of pole working height on failure probability.* As tower construction progresses, the working height of the pole will gradually enhance. Here, three working heights of the pole at 10 m, 20 m and 30 m are selected to explore the effect of pole working height on system failure. With the maximum wind speed of Vmax increasing from 25 m/s to 55 m/s, Figure 7 and Figure 8 present the variations of failure probabilities for the tower and the pole, respectively. For the tower, as displayed in Figure 7, its failure probability remains low level (less than

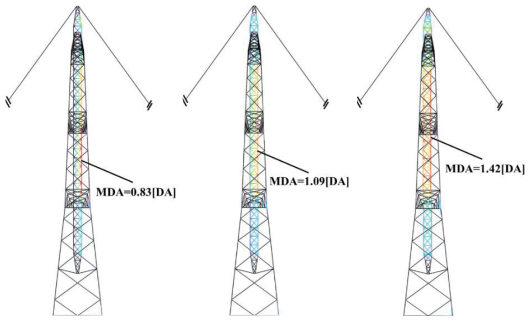

(A) LS1 (B) LS2 (C) LS3

FIGURE 6. Typical failure modes of the tower-pole system.

TABLE 5. Finite element analysis results of wind-induced responses at different working heights.

Working height of pole	Maximum stress (MPa)	Maximum displacement (mm)			
		Tower	Bottom of pole	Middle of pole	Top of pole
32	34.63	14.7	24.6	683.5	35.7
30	33.66	13.8	21.3	646.1	34.6
25	33.28	13.3	18.2	617.4	32.3
20	32.58	13.1	15.6	590.6	31.0
15	30.26	13.7	13.3	457.2	27.6

6% for LS1) as the wind speed increases up to 40 m/s. At the extreme wind speed of 55 m/s, the failure probability of the tower suffering from serious harm (LS2) approaches only 10%, indicating that the tower can maintain integral stability even under the action of strong winds. This outcome might be attributed to the excellent resistance to extreme wind loads designed for the transmission tower.

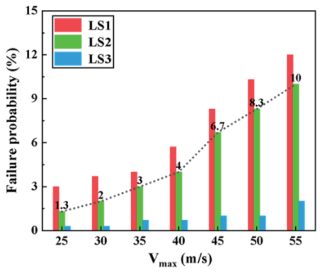

FIGURE 7. Variation of failure probability for the tower at working height of 30 m.

Different from the tower, the pole presents significantly higher failure probabilities under conditions of LS1 and LS2 as $V_{\max}$ gradually increases from 25 m/s to 55 m/s, and the working height has minimal influence on the failure probability of the pole, as shown in Figure 8(a) and (b). Specifically, the maximum failure probability of LS1 (see Figure 8(a)) reaches higher than 40% at $V_{\max} = 50m/s$ and then the failure probability begins to decline. This phenomenon could be attributed to the fact that, at higher wind speeds, some instances of minor harm are converted into

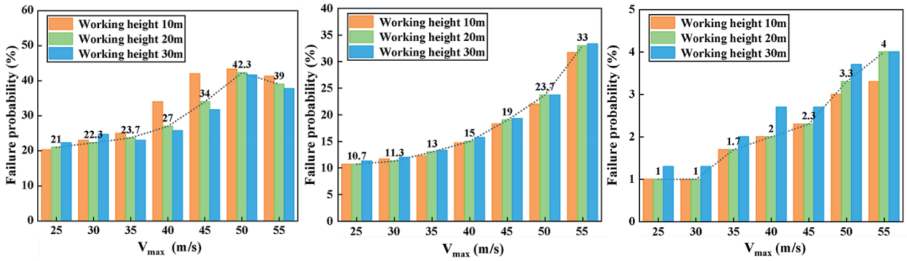

(A) LS1 (B) LS2 (C) LS3

FIGURE 8. Variation of failure probability of the pole under different wind speed.

serious harm, resulting in a significant increase in the failure probability of LS2 (see Figure 8(b)). At a working height of 20 m, the maximum failure probability of serious harm exceeds 33%, indicating that the pole can be considered to own sustained serious harm. For the complete harm in LS3 (see Figure 8(c)), however, the probability of failure is the lowest among the three harm levels and its maximum failure probability does not exceed 5% at $V_{\max} = 55m/s$, indicating that the pole investigated here would not be seriously damaged in downbursts. Of course, this outcome is in accordance with the definition of LS3 given in Eq. (3.6) and Table 3. As the displacement angle calculated at failure in LS3 is largest, which is 1.3 times [DA], it is hardest to reach the failure of complete harm in the pole. Therefore, the risk of failure in LS3 would be the lowest among the three harm levels.

Generally, Figure 8 reveals that downburst wind loads have a significant impact on the failure probability of the tower-pole system, particularly when Vmax exceeds 45 m/s. As expected, the progression from minor harm (LS1) to complete harm (LS3) also highlights an increasing severity of failure risk under downburst wind loads. Besides, taking the serious harm condition (LS2) and the control failure probability of 15% into account [14, 17], it can be derived from Figure 8(b) that the investigated tower-pole system can resist the wind loads with Vmax less than 40 m/s in downbursts. On the contrary, the downburst with Vmax larger than 45 m/s would become a wind condition with significant risk of failure. Therefore, $V_{\max} = 45m/s$ will be utilized to further analyze the system reliability when the vertical length and cross-section dimenions of the pole are changed.

4.2.2. *Effect of vertical length of pole on failure probability.* Considering the effects of different pole dimensions on the tower-pole system stability, this section modifies the vertical length of the pole (20 m, 24 m, 28 m and 32 m) to perform a failure probability comparison on the system under downbursts with $V_{\max} = 45m/s$. When the working height of the pole is maintained at 30 m, Figure 9 shows the comparative results in failure probability for four vertical lengths of the pole under conditions of LS1, LS2 and LS3. The outcomes presented in Figure 9 indicate that the failure probabilities of four investigated poles under three limit states are relatively similar, with shorter poles exhibiting only a marginal decrease in failure

probability compared to their longer counterparts. This phenomenon can be attributed to two main factors. Firstly, the maximum displacement required to reach the limit state enlarges with increasing the vertical length of pole. Secondly, an increase in vertical length of pole results in a corresponding increase in the self-weight of the pole, which would enhance its wind resistance. Consequently, keeping the cross-section dimension unchanged, the failure probabilities of the pole with various vertical lengths are closely aligned under the condition of downburst with $V_{\max} = 45m/s$. By comparison, it is recommended to select the shorter poles within the permissible limit of practical engineering, which may provide a slight enhancement in the wind resistance.

In some cases, the length of the pole cannot be changed during the construction process. Under this condition, the middle displacement of the pole can be controlled by adding the waist ring. Figure 10 shows the comparisons of maximum displacement and failure probabilities of the 28 m pole under the original case and the addition of a waist ring at middle height. It can be observed from Figure 10(a) that the maximum displacement of the pole is significantly reduced after using the waist ring constraint, which is only 1/3 of the original case. Therefore, adding the waist ring is an effective solution to combat downburst. As indicated in Figure 10(b), the failure probability of the pole would decrease obviously when the waist ring is added at 1/2 height of the pole. It can be proved that the effect of this constraint is better than that of shortening the pole length, and it is also more convenient to be utilized in the construction project.

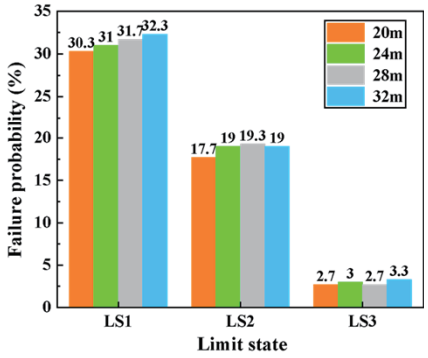

FIGURE 9. Failure probabilities of the pole with different vertical lengths.

4.2.3. *Effect of sectional area of pole element on failure probability.* To investigate the impact of the pole cross-sectional dimensions on the failure probability of the tower-pole system in downburst, the main components utilized in the 28 m pole are assumed to be changed from $\phi 45 \times 2.5$ to $\phi 65 \times 4$. Under the conditions of $V_{\max} = 45m/s$ and the pole working height of 30 m, the effect of the element cross-sectional areas on the failure probability of the pole is analyzed and the corresponding results under three limit states are illustrated in Figure 11.

From Figure 11, it can be observed that when the component cross-sectional area in the pole is relatively small, its resistance to extreme wind loads is inferior,

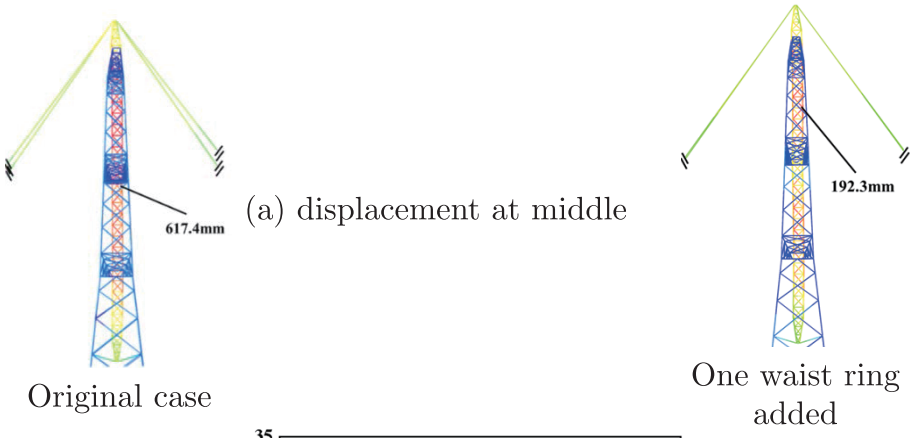

(a) displacement at middle

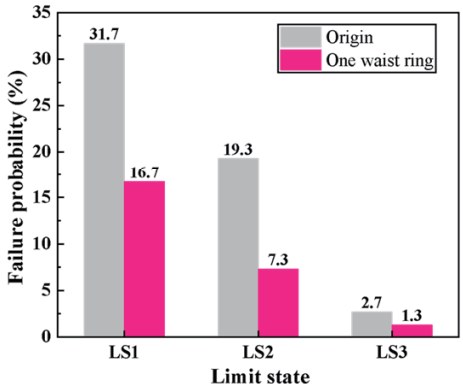

(b) failure probability

FIGURE 10. Comparisons of displacement and failure probabilities of the pole with or without waist ring.

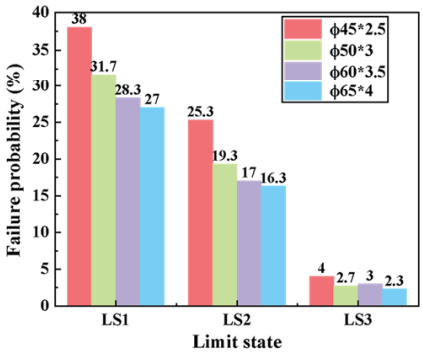

FIGURE 11. Failure probabilities of the pole with different element cross-sectional areas.

resulting in a higher failure probability across all limit states. Therefore, increasing the cross-sectional area of the pole can effectively enhance its wind resistance. On the other hand, it is important to note that an increase in cross-sectional sizes will lead to a further increase in the overall weight of the pole, thereby raising

construction costs and complicating installation procedures. A comparison of above results indicates that the investigated pole with the main elements of $\phi 50 \times 3$ steel pipes would be an appropriate pole to resist the downburst wind loads with $V_{\max} = 45m/s$.

5. Conclusions

Using the reliability theory, this study investigated the displacement failure probabilities of an under-construction transmission tower-pole system subjected to the extreme windy condition of downbursts. The main conclusions can be drawn as follows:

1) Downbursts would cause strong wind weather and their instantaneous wind speed can be calculated by a combination of mean wind speed and fluctuating wind speed. For the given values of $V_{\max}$ and $z_{\max}$, the downburst wind speed-time histories were introduced and compared. Through the analysis in wind speed frequency distribution, it is proposed to utilize the Fréchet distribution to describe the probability density function of downburst wind speed.
2) Based on the displacement control requirements, three successive limit states have been proposed to describe the damage degrees or performance levels of the tower-pole system exposed to downbursts. The maximum displacement angle (MDA) was utilized to evaluate the failure probability of the system.
3) A finite element model of this tower-pole system was established using ABAQUS software and its wind-induced responses were identified by applying quasi-static equivalent downburst wind loads. Latin Hypercube Sampling (LHS) method was employed to sample the random variables including downburst wind speed, geometric dimensions, and physical properties of elements, and accordingly the displacement related failure probabilities of the tower-pole system were calculated on three proposed limit states.
4) At a 90° direction angle of downburst winds, a case study indicates that the displacement responses in the tower-pole system are more remarkable than the stress responses, especially for the suspension pole. For three LSs, the failure probabilities occurred in the pole present different growth levels as the maximum wind speed of $V_{\max}$ increases from 25 m/s to 55 m/s. By comparison, it can be concluded that a high failure probability (higher than 15%) would occur in the pole under the conditions of LS1 and LS2. The current pole configuration with a vertical length of 28 m and the main elements of $\phi 50 \times 3$ steel pipes would be an appropriate pole to resist the downburst wind loads with $V_{\max} = 45m/s$.
5) The research results derived from this study not only provide a method of wind vibration response analysis and safety assessment for the under-construction transmission towers, but also provide a reference for the safety design of similar high-rise structures against severe wind loads. Considering the suddenness and strong destructive nature of extreme wind environments such as downbursts, however, the findings given in this study could not accurately represent the wind-induced responses and the failure risk of all types

of transmission towers under construction. Therefore, for a special under-construction transmission tower located in a certain area, further refined researches would also be required under downburst wind loads.

References

[1] A. Ahmed and A. E. Damatty, *Dynamic response of conductors during transmission tower failure under downburst loads*, Engineering Structures **305** (2024): 117727.

[2] E. S. Abd-Elaal, J. E. Mills and X. Ma, *A review of transmission line systems under downburst wind loads*, Journal of Wind Engineering and Industrial Aerodynamics**179** (2018), 503–513.

[3] American Society of Civil Engineers (ASCE), *Guidelines for Electrical Transmission Line Structural Loading (fourth ed.)*, USA: ASCE Manuals and Reports on Engineering Practice, 2020. https://ascelibrary.org/doi/pdf/10.1061/9780784415566.fm

[4] W. Bi, L. Tian, C. Li, H. Ma and P. Pan, *Wind-induced failure analysis of a transmission tower-line system with long-term measured data and orientation effect*, Reliability Engineering and System Safety **229** (2023): 108875.

[5] Canadian Standards Association/National Standard of Canada, *Design Criteria of Overhead Transmission Lines*, Canadian Standards Association, 2010. https://scc-ccn.ca/standards/notices-of-intent/csa-group/overhead-transmission-lines-design-criteria-1

[6] B. Chen, W.H. Guo, P. Y. Li and W. P. Xie, *Dynamic responses and vibration control of the transmission tower - line system: A state - of - the - art review*, The Scientific World Journal **1** (2014): 538457.

[7] L. Chen and C. W. Letchford, *A deterministic–stochastic hybrid model of downbursts and its impact on a cantilevered structure*, Engineering Structures **26** (2004), 619–629.

[8] A. E. Damatty and A. Elawady, *Critical load cases for lattice transmission line structures subjected to downbursts: economic implications for design of transmission lines*, Engineering Structures **159** (2018), 213–226.

[9] Z. Fang, Z. Wang, R. Zhu and H. Huang, *Study on wind-induced response of transmission tower-line system under downburst wind*, Buildings **12** (2022): 891.

[10] X. Fu, H.N. Li, L. Tian, J. Wang and H. Cheng, *Fragility analysis of transmission line subjected to wind loading*, Journal of Performance of Constructed Facilities **33** (2019): 04019044.

[11] National Standard of the People's Republic of China, GB 50068-2018, *Unified standard for reliability design of building structures*, Beijing, 2023. https://www.chinesestandard.net/PDF.aspx/GB50068-2018

[12] Ministry of Housing and Urban-Rural Development of the People's Republic of China, GB 50135-2019, *Standard for Design of High-rising Structures*. 2019. https://www.scribd.com/document/686658679/GB-50135-2019-Standard-for-Design-of-High-rising-Structures

[13] Joint Committee on Structural Safety (JCSS), JCSS-2001, *Probabilistic model code: Part 3-Resistance models[S]*. Denmark, 2001. https://www.jcss-lc.org/publications/jcsspmc/part_iii.pdf

[14] S. J. Kwon, U. J. Na, S. S. Park and S. H. Jung, *Service life prediction of concrete wharves with early-aged crack: Probabilistic approach for chloride diffusion*, Structural Safety **31** (2009), 75–83.

[15] X. Lei, X. Fu, K. Xiao, J. Wang, M. Nie, H. Li and W. Xie, *Failure analysis of a transmission tower subjected to wind load using uncertainty method*, Proceedings of the Chinese Society of Electrical Engineering **38** (2018), 266–274.

[16] S. Liu, W. Zhang, Q. Li, S. Yan, S. Zhang, C. Li and L. Li, *Engineering method for quantifying the coupling effect of transmission tower-line system under strong winds*, Journal of Wind Engineering & Industrial Aerodynamics, **255** (2024): 105954.

[17] C. H. Lu, W.L. Jin and R. G. Liu, *Probabilistic lifetime assessment of marine reinforced concrete with steel corrosion and cover cracking*, China Ocean Engineering **25** (2011), 305–318.

[18] L. Ma, M. Khazaali and P. Bocchini, *Component-based fragility analysis of transmission towers subjected to hurricane wind load*, Engineering Structures **242** (2021): 112586.
[19] N. P. Rao, G. M. S. Knight, S. J. Mohan and N. Lakshmanan, *Studies on failure of transmission line towers in testing*, Engineering Structure **35** (2012), 55–70.
[20] A. A. Saddek, T. K. Lin and W. L. A. Sawadogo, *Failure evaluation of transmission tower with asymmetrical legs by Scaled–Down pushover experiment*, Engineering Structures **279** (2023): 115511.
[21] A. Shehata and A. E. Damatty, *Extensible catenary approach in analyzing transmission line's conductors under downbursts*, Engineering Structures **234** (2021): 111905.
[22] A. Shehata and A. E. Damatty, *Numerical model of cascade failure of transmission lines under downbursts*. Engineering Structures **255** (2022): 113876.
[23] L. Tian, H. Pan, R. Ma, L. Zhang and Z. Liu.*Full-scale test and numerical failure analysis of a latticed steel tubular transmission tower*, Engineering Structures **208** (2020): 109919.
[24] D. D. Vicroy.*Assessment of microburst models for downdraft estimation*, Journal of Aircraft **29** (1992), 1043–1048.
[25] D. Wang, L. Yang, Y. Xiang, C. Sun and Q. Chen.*Analytical prediction of quasi-static responses of transmission lines under moving downbursts: A nonlinear model with linear approximation*, Journal of Wind Engineering & Industrial Aerodynamics **237** (2023): 105407.
[26] J. Zhang and Q. Xie, *Failure analysis of transmission tower subjected to strong wind load*, Journal of Constructional Steel Research **160** (2019), 271–279.
[27] Y. Zhang, D. Wang, C. Sun, X. Fu, *Probabilistic study on non-stationary extreme response of transmission tower under moving downburst impact*, Structures **68** (2024): 107179.
[28] H. D. Zheng and J. Fan, *Progressive collapse analysis of a truss transmission tower-line system subjected to downburst loading*, Journal of Constructional Steel Research, **188** (2022): 107044.
[29] C. Zhu, Q. Yang, G. Huang, X. Zhang and D. Wang, *Fragility analysis and wind directionality-based failure probability evaluation of transmission tower under strong winds*, Journal of Wind Engineering & Industrial Aerodynamics **246** (2024): 105668.
[30] X. Zhu and G. Ou, *Wind fragility modeling of transmission tower-line system based on threat-dependent structural robustness index*, Structural Safety **114** (2025): 102571.

Manuscript received October 24, 2024
revised February 19, 2024

X. Liu
State Grid Jiangsu Electric Power Co., Ltd. Construction Branch, Nanjing Jiangsu 210011, China
E-mail address: jackyone1981@yeah.net

T. Huang
State Grid Jiangsu Electric Power Co., Ltd. Construction Branch, Nanjing Jiangsu 210011, China
E-mail address: 2254017015@qq.com

Z. Liu
State Grid Jiangsu Electric Power Co., Ltd. Construction Branch, Nanjing Jiangsu 210011, China
E-mail address: 15951015099@163.com

J. Zhu
State Grid Jiangsu Electric Power Co., Ltd. Construction Branch, Nanjing Jiangsu 210011, China
E-mail address: zhujiao90@163.com